

Published in final edited form as:

Nature. 2011 March 31; 471(7340): 656–660. doi:10.1038/nature09795.

Crystal structure of constitutively active rhodopsin: How an agonist can activate its GPCR

Jörg Standfuss^{1,2}, Patricia C. Edwards¹, Aaron D'Antona³, Maikel Fransen¹, Guifu Xie³, Daniel D. Oprian³, and Gebhard F. X. Schertler^{1,2,4}

¹MRC Laboratory of Molecular Biology, Hills Road, Cambridge CB2 0QH, UK ²Paul Scherrer Institut, Villigen PSI, 5232, Switzerland ³Department of Biochemistry and Volen Center for Complex Systems, Brandeis University, Waltham 02454, USA

Abstract

G protein-coupled receptors (GPCRs) comprise the largest family of membrane proteins in the human genome and mediate cellular responses to an extensive array of hormones, neurotransmitters, and sensory stimuli. While some crystal structures have been determined for GPCRs, most are for modified forms, showing little basal activity, and are bound to inverse agonists or antagonists¹. Consequently, these structures correspond to receptors in their inactive states. The visual pigment rhodopsin is the only GPCR for which structures exist that are thought to be in the active state^{2,3}. However, these structures are for the apoprotein or opsin form that does not contain the agonist all-*trans* retinal.

We present here a crystal structure for the constitutively active rhodopsin mutant E113Q⁴⁻⁶ in complex with a peptide derived from the C-terminus of the G protein transducin (the GaCT peptide). Importantly, the protein appears to be in an active conformation, and retinal is retained in the binding pocket after photoactivation. Comparison with the structure of ground state rhodopsin⁷ suggests how translocation of the retinal β -ionone ring leads to a rotational tilt of transmembrane helix 6 (TM6), the critical conformational change upon activation⁸. A key feature of this conformational change is a reorganization of water mediated hydrogen-bonding networks between the retinal-binding pocket and three of the most conserved GPCR sequence motifs. For the first time we thus show how an agonist ligand can activate its GPCR.

In the dark, rhodopsin contains a covalently bound 11-*cis*-retinal chromophore that preferentially binds to the inactive state and therefore functions as an inverse agonist in the visual system. Upon exposure to light, the retinal isomerizes to the all-*trans*-form, initiating a series of conformational changes leading to the transient intermediate metarhodopsin-II (meta-II), responsible for activating the G protein. All-*trans*-retinal thus functions in this scenario as an agonist for activation of the receptor.

The first structures of bovine rhodopsin were determined for the inactive-state of the native protein bound to the 11-*cis*-retinal chromophore⁹. Other dark-state structures followed^{7,10}, including those for rhodopsin containing non-native 9-*cis*-retinal¹¹ and squid rhodopsin¹². Importantly, several structures have been determined for crystals of the protein following photoisomerisation of the chromophore to the all-*trans*-form¹³. However, these are thought to be for early photointermediates in the activation pathway and have not yet undergone the critical conformational alteration required for activation of the G protein.

⁴Corresponding Author to whom correspondence should be addressed: Prof. Gebhard F. X. Schertler, Paul Scherrer Institut, Villigen PSI, 5232 Switzerland Tel: +41-56-310-4265, Fax: +41-56-310-5288 Gebhard.Schertler@psi.ch.

Recently, two structures thought to represent the active state have been determined for the apoprotein form opsin^{2,3}. The two structures are very similar and are thought to represent activated forms of the receptor because one was determined for opsin bound to a peptide derived from the C-terminal tail of the α -subunit of the G protein transducin (G α CT) known to bind preferentially and stabilize the active intermediate meta-II¹⁴. While the opsin structures are of immense value to our understanding of the active state, a complete understanding of the active state will require structures in which the all-*trans*-retinal agonist is included in the ligand-binding pocket of the receptor.

In an attempt to obtain active-state crystals of rhodopsin, which still contain the all-*trans*-retinal ligand, we used the crystallization conditions described for opsin but substituted a previously described mutant, E113Q^{3,28} (superscripts denote the Ballesteros-Weinstein general GPCR numbering), for the native protein. E113Q^{3,28} incorporates a change of the Schiff base counterion^{4,5}, and there were three reasons for choosing it for these studies. First, hydrolysis and dissociation of all-*trans*-retinal from the photoactivated protein is dramatically slowed in the mutant⁵. Second, fourier transform infrared spectroscopy (FTIR) shows that the mutant lacks a classical meta-I/meta-II equilibrium, instead favouring the active meta-II state, and that the normally inactive post-meta-II intermediate meta-III is in fact in an active conformation¹⁵. Third, the opsin form of the E113Q^{3,28} mutant is constitutively active⁶, and addition of all-*trans*-retinal to the apoprotein can activate the mutant to levels comparable to those of light-activated wild-type rhodopsin^{5,16}, essentially turning rhodopsin into a GPCR that binds and is activated by diffusible agonists. Unfortunately, the E113Q^{3,28} mutant is also significantly less stable than wild-type rhodopsin (Supplementary Figure 1), and for this reason we used the E113Q mutation in the context of another rhodopsin mutant, N2C/D282C, containing an engineered disulfide bond known to enhance thermal stability of the protein without affecting activity^{15,17}. We previously solved the structure of this stabilized mutant and showed it to be virtually identical with that of the native protein with the important exceptions that the oligosaccharide chain normally linked to Asn2 is missing, and the two engineered Cys residues are linked by a disulfide bond¹⁸.

The E113Q/N2C/D282C triple mutant (henceforth referred to as simply the E113Q^{3,28} mutant) was expressed and purified using a previously described immunoaffinity procedure in which rhodopsin is reconstituted with 11-*cis*-retinal while still immobilized on the affinity matrix¹⁸. The purified protein was then mixed with lipids and the G α CT peptide before light was used to isomerise retinal and activate the protein just before crystallization. In independent experiments, crystals were also grown in the dark from E113Q^{3,28} opsin in the presence of all-*trans*-retinal. Crystals from both samples displayed a faint yellow colour (Supplementary Figure 2) indicative of bound retinal. While complete data sets were generated from both samples, we present data obtained from light-activated rhodopsin as selective illumination of protonated retinal minimises formation of unwanted isomers and resembles activation in the retina more closely.

The structure, solved by molecular replacement, contains residues 1-326 of the mutant opsin and all eleven residues of the G α CT peptide, including the Lys341 \rightarrow Leu mutation introduced to increase affinity for the receptor¹⁹. In addition, clear electron density is observed for two partially ordered lipid molecules, one molecule of octylglucoside, several previously unresolved water molecules, and most strikingly, retinal within the ligand-binding pocket of the receptor (see below). With the exception of the missing oligosaccharyl chain at position 2, the recombinantly produced protein contains all post-translational modifications observed with the native protein purified from bovine retina including acetylation of the N-terminus, palmitoylation of Cys residues at positions 322 and 323, and

glycosylation of Asn at position 15. Finally, the engineered disulfide between Cys residues at positions 2 and 282 is clearly visible in the mutant.

The structure of the E113Q/GαCT complex deviates significantly from the ground-state structure of rhodopsin (1GZM)⁷, but displays high similarity to the active-state structure of the opsin/GαCT complex (3DQB)³, with respective Ca RMS deviations of 2.42 Å and 0.58 Å (supplementary Figure 3). The E113Q/GαCT structure is also in good agreement with the results of high-resolution distance mapping using double-electron-electron resonance (DEER) spectroscopy to investigate movement undergone by rhodopsin in the photoactivation event where pairs of nitroxide spin labels (in particular at positions 241 and 252) were used to quantify a 5-Å outward movement of TM6 critical to the activation process²⁰. For comparison, the Ca atoms of Arg241^{6,42} and Ala252^{6,35} of TM6 in the E113Q/GαCT structure are shifted by 5.1 Å and 4.1 Å, respectively, with regard to the same reference point within ground-state rhodopsin used in the DEER experiments (supplementary Table1), providing excellent agreement with the biophysical studies. Other residues not showing significant change in the DEER experiments also do not show significant difference from ground-state rhodopsin in the E113Q/GαCT structure.

On the basis of constitutive activity of the E113Q^{3,28} mutant, presence of the GαCT peptide in the structure, and agreement with the results from DEER spectroscopy, we conclude that the structure of the E113Q/GαCT complex reported here is in fact that of the active state.

As is shown in Figure 1, electron density for retinal is clearly observed in the general area where 11-*cis*-retinal is found in ground-state rhodopsin, confirming the presence of the chromophore in the ligand-binding pocket of the E113Q/GαCT complex. However, density for the nearby side-chain of Lys296^{7,43} is weak indicating that retinal is not bound to the protein covalently by a Schiff base, as in ground-state rhodopsin or the meta-II state. In addition, density for the β-ionone ring and most of the polyene chain is well defined but broadens after position C9 suggesting that the retinal is present as a mixture of isomers. We have modelled retinal in the all-*trans* conformation, but based on occupancy refinement we estimate a mixture composed of 60% all-*trans*-retinal and 40% of various isoforms. However, it is important to note that we cannot distinguish between a model based upon a mixture of *cis* and *trans* isomers about double bonds, catalyzed for example by phosphatidylethanolamine lipids²¹ or Lys296^{7,43}, and one based upon a mixture of conformers arising from rotations about single bonds in the polyene chain. In fact, the latter might be more likely as similar electron density was observed for the retinal in crystals grown from E113Q^{3,28} opsin and all-*trans*-retinal in the dark, in this case the chromophore never having been exposed to light.

These conclusions, that retinal is bound non-covalently to the protein and that it is composed of a mixture of isomers, are rather surprising as E113Q^{3,28} is known to contain a covalently bound all-*trans*-retinal ligand under similar conditions in solution studies^{4,5}. Clearly, the structure represents an active conformation but is not identical to metarhodopsin-II because the covalent bond to Lys296^{7,43} is not present. We suspect that it probably corresponds to a trapped intermediate in which the retinal is either entering or exiting the ligand-binding pocket. It is well established that wild-type opsin transiently activates as retinal enters the binding pocket but before a covalent bond to Lys296^{7,43} has been formed²², and that both all-*trans* and 11-*cis* retinol can act as potent agonists²³. In this regard, the ionone ring-end of retinal and part of the polyene chain in the E113Q/GαCT structure is probably in the same position that it occupies in meta-II despite the absence of a covalent bond to Lys296^{7,43}. The location of the β-ionone ring is shifted 4.3 Å from its position in ground-state rhodopsin (Figure 1) and inserted in the cleft between TM5 (residues Met207^{5,42}, Phe208^{5,43}, and Phe212^{5,47}) and TM6 (residues Trp265^{6,48}, Ala269^{6,52}, and Ala272^{6,55}). This position is in

excellent agreement with (2D) dipolar-assisted rotational resonance (DARR) NMR experiments of the retinal position in the meta-II state²⁴.

The transition from inactive to active states evident upon comparison of the ground-state and active-state structures is accompanied by global rearrangement of the seven transmembrane helix bundle (Figure 2) that produces an apparent tilt of the cytoplasmic end of TM6 (and to a lesser extent TM5) away from the bundle core (TM1-TM4 and TM7). The apparent tilt is not achieved through a hinge movement but by rotation about the main axis of TM6 that leaves the shape of the helix intact. On the cytoplasmic side, the rotational tilt is amplified through the characteristic bend caused by Pro267^{6,50}, the most conserved residue in TM6 among GPCRs and part of the ubiquitous CWxP motif. Pro267^{6,50} is in close contact with water7 that is hydrogen bonded to Cys264^{6,47}, Tyr268^{6,51}, and Pro291^{7,38}, an arrangement similar to that observed in ground-state rhodopsin. This water is found also in structures of the beta1 adrenergic, beta2 adrenergic, and adenosine receptors, and likely forms an important architectural element in formation of the bend in TM6.

Trp265^{6,48} of the CWxP motif is a highly conserved amino acid that is tightly packed against retinal in ground-state rhodopsin and has been identified as important for GPCR activation through early mutagenesis studies. Trp265^{6,48} occupies a central role in the toggle-switch model for activation of GPCRs²⁵ and, in rhodopsin, is thought to be released by *cis/trans* isomerisation of the chromophore allowing H6 to swing out and expose the G protein-binding site^{7,24}. Superposition of the ground-state (1GZM) and E113Q/GαCT structures indicates that the indole group of Trp265^{6,48} has moved 3.6 Å away from its ground-state position as a consequence of rhodopsin activation. However, we do not observe the rotamer change that has been originally proposed based on computer simulations. Instead, Trp265^{6,48} follows the β-ionone ring, maintaining contact with the C18 methyl group. Importantly, the spectral changes measured for Trp265^{6,48} by DARR spectroscopy²⁴ are in good agreement to the movement of Trp265^{6,48} revealed by our structure, which involves a translation without rotation of the side chain. It is tempting then to suggest that the critical movement of TM6 stems from a motion of the β-ionone ring against TM6 just beneath the CWxP motif, while Trp265^{6,48} is simultaneously released from its locked ground-state position.

Of special interest in the E113Q/GαCT structure is a cluster of densities that indicate the presence of structural water molecules (Figure 3) between some of the most conserved residues in GPCRs. While modelling of water is difficult in the 3Å resolution range, omission of this potential water cluster during refinement resulted in clear difference peaks (panel A), presumably due to tight hydrogen bonding typical for structural waters in the interior of membrane proteins. Our interpretation of these difference peaks as waters is further strengthened by the presence of a similar hydrogen-bonding network found in ground state rhodopsin that begins at Trp265^{6,48}, involves the conserved Asp83^{2,50} in TM2 and Ser298^{7,45} and Asn302^{7,49} (of the NPxxY motif) in TM7, and ends just below a hydrophobic barrier formed by six residues (Leu76^{2,43} and Leu79^{2,46} in TM2; Leu128^{3,43} and Leu131^{3,46} in TM3; Met253^{6,36} and Met257^{6,40} in TM6), of which many are conserved in rhodopsin-class GPCRs.

The E113Q/GαCT structure indicates a rearrangement of this water cluster through rotation of TM6. The water-mediated link between Trp265^{6,48} in TM6 and Ser298^{7,45} in TM7 is broken, while Ser298^{7,45} together with water16, Asn55^{1,50}, Asp83^{2,50} and Asn302^{7,49} continues to stabilize the unusual Pro-kink introduced in TM7²⁶ by Pro303^{7,50}. While these reorganizations are comparatively minor, they directly link changes in the CWxP motif in the retinal-binding pocket with the two most conserved residues in TM1 and TM2, and the NPxxY motif in TM7. On the cytoplasmic site of the reorganized hydrogen-bonding

network, the rotation of TM6 in the activated state breaks the hydrophobic barrier between the retinal- and G protein-binding sites. Two conserved residues, Tyr223^{5,58} of TM5 and Tyr306^{7,53} of the NPxxY motif, swing into the protein interior from their membrane-facing positions in the ground state to fill the gap created by removal of Met257^{6,40}. The phenolic side chains allow additional interactions with water molecules (waters 2+14) and extension of the hydrogen-bonding network through the opened hydrophobic barrier up to the highly conserved E(D)RY motif at the cytoplasmic surface of TM3. Residue Glu134^{3,49} and Arg135^{3,50} of this motif are released from the bent conformation in the ground state, which opens the ionic lock interactions²⁷ of Glu134^{3,49}/Arg135^{3,50} and Glu247^{6,30} and allows binding of the G protein peptide in a position that is occupied by TM6 in the ground state. Thus, rotation of TM6 and displacement of Trp265^{6,48} results in a hydrogen-bonding network connecting residues from the protein interior in contact with retinal to those at the cytoplasmic surface critical to activation of the G protein. The hydrogen-bonding network is further extended towards the G α CT peptide by water13 bridging Tyr306^{7,53} and Arg135^{3,50} to Asn310^{8,47} in the TM7-H8 junction (Figure 3). Asn310^{8,47} in turn interacts with water9, which forms hydrogen bonds to Asn73^{2,40} of the receptor and the backbone carbonyl of Asp346 in the G α CT peptide. Asp346 of the peptide appears to be a key residue for binding as the backbone carbonyl is linked to Thr70^{2,37} of cytoplasmic loop1 through water8, and the side chain is linked to Asn343 of the peptide and Arg147^{3,62} of the receptor through water5.

This newly recognized extension of the water mediated hydrogen-bonding network provides a beautiful structural context (Figure 4) for interpretation of results from several biochemical studies. First, mutations of L79^{2,46}, Glu134^{3,49}, Arg135^{3,50} and Met257^{6,40} are known to strongly favour the meta-II state or constitutively activate rhodopsin. Second, the active-state reorganization of the cytoplasmic ends of TM3, TM6 and TM7 connecting three of the most conserved sequence motifs in GPCRs is expected to be restrained by a salt bridge between Glu113^{3,28} and Lys296^{7,43}; mutation of either residue leads to constitutive activation⁶. Third, the rhodopsin double mutant Y306C/F313C is unable to form meta-II under oxidizing conditions but does so under reducing conditions, albeit with severely reduced ability to activate the G protein²⁸. Finally, mutation of Tyr227^{5,58} in the beta1 adrenergic receptor (Tyr223^{5,58} in rhodopsin) to Ala leads to strong stabilization of the antagonist binding conformation, an effect that has been attributed to an impaired ability to form the inherently less stable active conformation²⁹.

In summary, we describe here how translocation of the retinal β -ionone ring can lead to the conformational changes that allow rhodopsin to bind its G protein. For the first time we show how an agonist is bound to the active state of a GPCR and how activation is accompanied by a reorganization of hydrogen-bonding networks between some of the most conserved residues among GPCRs. Additional structures of activated GPCRs, and their thorough analysis using structural bioinformatics tools will show to which extent this activation mechanism is conserved throughout this important class of signal transducers comprising more than 1% of the human genome.

Materials and Methods

Preparation of stable cell line

The rhodopsin gene containing the stabilizing N2C/D282C and E113Q counterion mutation was cloned into the pACMVtetO vector for tetracycline-inducible expression in mammalian cells³⁰ using NotI and KpnI restriction sites. HEK293S-GnTI⁻ cells with restricted and homogenous N-glycosylation were stably transfected with this vector as described³¹. Both vector and cells were a kind gift from Philip J. Reeves, University of Essex, UK.

Large-scale expression in wave bag bioreactors

Cells were expanded as adhesion cultures in DMEM/F12 medium supplemented with FBS (10%), PenStrep (Gibco), Geneticin-G418 (200 μ g/ml) and blasticidin (5 μ g/ml). Cells from 5 fully confluent 75cm² flasks were harvested and further expanded into a 300ml suspension culture in Freestyle Medium (Invitrogen) supplemented with FBS (5%) and PenStrep (Gibco). A wave bioreactor (GE Healthcare) was used to further expand the initial suspension cultures to a volume of 9.5l with a cell density of 2 \times 10⁶ cells per millilitre. Protein expression was induced by 0.5l medium supplemented with tetracycline and sodium butyrate for final concentrations in the wave bag of 2 μ g/ml and 5mM. Cells were harvested 72h after induction at a density of 4-5 \times 10⁶ cells per millilitre. Cell pellets were washed with PBS buffer containing protease inhibitor cocktail (complete protease inhibitor cocktail tablets, Roche) and stored at -80°C. The modelled N-glycan in the final structure is based on the homogenous glycosylation pattern of the HEK293-GnTI⁻ cell line³¹ used for expression and has been built as GlcNAc₂-Man₃ with two disordered mannose sugars. Crystal contacts between two N-glycans and palmitoyl chains that fill the cavity between the two rhodopsin molecules in the crystallographic dimer suggest the homogeneous posttranslational modifications as an important factor in crystal formation.

Purification

Cell pellets were solubilized for 1 hour at 4°C with PBS buffer containing protease inhibitor tablets (complete protease inhibitor cocktail tablets, Roche) and 1.25% DM (β -decyl-maltoside). Nuclei and other unsolubilized material were removed by centrifugation and the supernatant incubated with 1D4 antibody coupled to CnBr activated sepharose (Amersham Biosciences). After 3-4 hours the matrix was washed with PBS pH 7, 0.125% DM. Ground state rhodopsin was reconstituted by adding 11-*cis* retinal (50 μ M) to the matrix and overnight incubation at 4°C. All steps involving retinal were performed under dim red light.

The matrix was washed with PBS pH 7.0, 0.125% DM followed by 10mM Hepes pH 7.0, 1% OG (β -octyl-glycoside). The purified protein was eluted in the same buffer supplemented with an elution peptide resembling the C-terminus of rhodopsin (TETSQVAPA, 80 μ M). The eluate was reduced to 0.5ml by a 50kD cutoff concentrator prior to gel filtration on a Superdex200 column. The gel filtration step was used to exchange the buffer for 10mM Mes pH 5.0, 100mM NaCl, 1% OG which leads to protonation of the Schiff base in the E113Q counterion mutant and shifts the absorption maximum from 382nm to 498nm^{4,5,15}.

Light activation and crystallization

Reconstituted E113Q was concentrated to 5-7.5 mg/ml (Vivaspin, 50kD cutoff concentrator) and mixed with dried brain lipid extract (Avanti Polar Lipids, 1 w/w, 10 μ M all-trans retinal). The sample was briefly sonicated and incubated for 30 minutes in presence of a 10 fold molar excess of peptide resembling the last eleven amino-acids of the G α subunit of the G protein carrying the mutation K341L (ILENLKDCGLF, Advanced Biomedical). The receptor was activated with for 5 minutes using a >515nm long pass filter that prevented light exposure of free retinal and meta-II.

Sample was mixed 1:1 with 3.0-3.4 M ammonium sulphate, 100 mM sodium acetate pH 4.5 and crystallized by sitting drop vapour diffusion in the dark. Crystals were harvested under dim-red light and soaked in crystallization buffer containing 10% trehalose prior to freezing in liquid nitrogen.

Data Collection and Structure determination

Diffraction quality of crystals was assessed at several synchrotron X-ray sources (SLS, Villigen, ESRF, Grenoble and DIAMOND, Didcot). The best data with a maximum resolution of 2.9Å was collected at the micro-focus beamline ID23eh-2 (ESRF, Grenoble) by the helical data collection method. Data were integrated using XDS³² and brought onto a common scale using SCALA from the CCP4 program suite³³. Dataset statistics are given in supplementary table 2.

Phases were obtained by molecular replacement using the program PHASER³⁷ and the polypeptide of the opsin structures (3CAP² and 3DQB³) or the ground state rhodopsin structure (1GZM⁷) as search model. The resulting solution was refined using iterative cycles of model building in COOT³⁴ and refinement (rigid body, energy minimization, simulated annealing, individual B-factor refinement) with the PHENIX program suite³⁵. Ordered water molecules were added to the model based on five criteria. First, clear difference peaks in a 2.5 sigma contoured Fo-Fc electron density map calculated after simulated annealing refinement in which water molecules have been omitted (Figure 3). Second, density above 1 sigma in 2Fo-Fc maps refined including waters. Third, two or more hydrogen bonds to the protein or other water molecules. Fourth, a B-factor cutoff within 20% of the average and finally, interpretable density in maps calculated with both datasets.

Geometric restraints for lipids and heteroatoms were prepared using the PRODRG2 server³⁸ (<http://davapc1.bioch.dundee.ac.uk/prodrg/>) and Hic-Up database³⁹ (<http://xray.bmc.uu.se/hicup/>). Coordinates for all-*trans* and 9-*cis* retinal were obtained from the Cambridge Small Molecule Database. Retinal geometry restraints used in the refinement were prepared by carefully adjusting torsion angles and planarity restraints in the retinal parameter file distributed as part of the CCP4 program suite. Coordinates and structure factors have been deposited under pdb code 2x72 in the case of light activated E113Q rhodopsin and xxxx of constitutively active opsin.

Supplementary Material

Refer to Web version on PubMed Central for supplementary material.

Acknowledgments

We thank Phil Evans, Xavier Deupi and Reiner Vogel for discussions and reading of the manuscript. We thank Rosalie Crouch at the University of South Carolina for the kind gift of 11-*cis* retinal. Phil J. Reeves at the University of Essex we thank for providing the pACMVtetO vector and the HEK293S-GnTI⁻ cells and for his advice on creating stable cell lines and tetracycline-inducible expression. We also thank staff at the macromolecular crystallography beamlines at the European Synchrotron Radiation Facility (ESRF), the Diamond Light Source and the Swiss Light Source (SLS). The work was financially supported by NIH grant EY007965 (to D.O.), the Human Frontier Science Project (HFSP) program grant RG/0052 (to D.O. and G.S.), the European Commission FP6 specific targeted research project LSH-2003-1.1.0-1 (to G.S.), the Marie Curie Intra European Fellowship MEIF-CT-2006-039171 (to J.S.) and the EMBO long-term fellowship ALTF 198-2006 (to J.S.).

Abbreviations

GPCR	G protein-coupled receptor
TM	transmembrane helices
meta	metarhodopsin
GαCT	peptide derived from the C terminus of the G protein α subunit

References

1. Rosenbaum DM, Rasmussen SG, Kobilka BK. The structure and function of G-protein-coupled receptors. *Nature*. 2009; 459(7245):356. [PubMed: 19458711]
2. Park JH, et al. Crystal structure of the ligand-free G-protein-coupled receptor opsin. *Nature*. 2008; 454(7201):183. [PubMed: 18563085]
3. Scheerer P, et al. Crystal structure of opsin in its G-protein-interacting conformation. *Nature*. 2008; 455(7212):497. [PubMed: 18818650]
4. Zhukovsky EA, Oprian DD. Effect of carboxylic acid side chains on the absorption maximum of visual pigments. *Science*. 1989; 246(4932):928. [PubMed: 2573154]
5. Sakmar TP, Franke RR, Khorana HG. Glutamic acid-113 serves as the retinylidene Schiff base counterion in bovine rhodopsin. *Proc Natl Acad Sci U S A*. 1989; 86(21):8309. [PubMed: 2573063]
6. Robinson PR, Cohen GB, Zhukovsky EA, Oprian DD. Constitutively active mutants of rhodopsin. *Neuron*. 1992; 9(4):719. [PubMed: 1356370]
7. Li J, et al. Structure of bovine rhodopsin in a trigonal crystal form. *J Mol Biol*. 2004; 343(5):1409. [PubMed: 15491621]
8. Farrens DL, et al. Requirement of rigid-body motion of transmembrane helices for light activation of rhodopsin. *Science*. 1996; 274(5288):768. [PubMed: 8864113]
9. Unger VM, Hargrave PA, Baldwin JM, Schertler GF. Arrangement of rhodopsin transmembrane alpha-helices. *Nature*. 1997; 389(6647):203. [PubMed: 9296501] Palczewski K, et al. Crystal structure of rhodopsin: A G protein-coupled receptor. *Science*. 2000; 289(5480):739. [PubMed: 10926528]
10. Okada T, et al. The retinal conformation and its environment in rhodopsin in light of a new 2.2 Å crystal structure. *J Mol Biol*. 2004; 342(2):571. [PubMed: 15327956]
11. Nakamichi H, Buss V, Okada T. Photoisomerization mechanism of rhodopsin and 9-cis-rhodopsin revealed by x-ray crystallography. *Biophys J*. 2007; 92(12):L106. [PubMed: 17449675]
12. Murakami M, Kouyama T. Crystal structure of squid rhodopsin. *Nature*. 2008; 453(7193):363. [PubMed: 18480818]
13. Ruprecht JJ, et al. Electron crystallography reveals the structure of metarhodopsin I. *EMBO J*. 2004; 23(18):3609. [PubMed: 15329674] Salom D, et al. Crystal structure of a photoactivated deprotonated intermediate of rhodopsin. *Proc Natl Acad Sci U S A*. 2006; 103(44):16123. [PubMed: 17060607] Nakamichi H, Okada T. Local peptide movement in the photoreaction intermediate of rhodopsin. *Proc Natl Acad Sci U S A*. 2006; 103(34):12729. [PubMed: 16908857]
14. Hamm HE, et al. Site of G protein binding to rhodopsin mapped with synthetic peptides from the alpha subunit. *Science*. 1988; 241(4867):832. [PubMed: 3136547] Vogel R, Siebert F. Conformations of the active and inactive states of opsin. *J Biol Chem*. 2001; 276(42):38487. [PubMed: 11502747]
15. Standfuss J, Zaitseva E, Mahalingam M, Vogel R. Structural impact of the E113Q counterion mutation on the activation and deactivation pathways of the G protein-coupled receptor rhodopsin. *J Mol Biol*. 2008; 380(1):145. [PubMed: 18511075]
16. Cohen GB, Oprian DD, Robinson PR. Mechanism of activation and inactivation of opsin: role of Glu113 and Lys296. *Biochemistry*. 1992; 31(50):12592. [PubMed: 1472495]
17. Xie G, Gross AK, Oprian DD. An opsin mutant with increased thermal stability. *Biochemistry*. 2003; 42(7):1995. [PubMed: 12590586]
18. Standfuss J, et al. Crystal structure of a thermally stable rhodopsin mutant. *J Mol Biol*. 2007; 372(5):1179. [PubMed: 17825322]
19. Martin EL, Rens-Domiano S, Schatz PJ, Hamm HE. Potent peptide analogues of a G protein receptor-binding region obtained with a combinatorial library. *J Biol Chem*. 1996; 271(1):361. [PubMed: 8550587]
20. Altenbach C, et al. High-resolution distance mapping in rhodopsin reveals the pattern of helix movement due to activation. *Proc Natl Acad Sci U S A*. 2008; 105(21):7439. [PubMed: 18490656]
21. Groenendijk GW, Jacobs CW, Bonting SL, Daemen FJ. Dark isomerization of retinals in the presence of phosphatidylethanolamine. *Eur J Biochem*. 1980; 106(1):119. [PubMed: 7341223]

22. Kefalov VJ, Crouch RK, Cornwall MC. Role of noncovalent binding of 11-cis-retinal to opsin in dark adaptation of rod and cone photoreceptors. *Neuron*. 2001; 29(3):749. [PubMed: 11301033]
23. Kono M, Goletz PW, Crouch RK. 11-cis- and all-trans-retinols can activate rod opsin: rational design of the visual cycle. *Biochemistry*. 2008; 47(28):7567. [PubMed: 18563917]
24. Ahuja S, et al. Location of the retinal chromophore in the activated state of rhodopsin*. *J Biol Chem*. 2009; 284(15):10190. [PubMed: 19176531]
25. Shi L, et al. Beta2 adrenergic receptor activation. Modulation of the proline kink in transmembrane 6 by a rotamer toggle switch. *J Biol Chem*. 2002; 277(43):40989. [PubMed: 12167654] Schwartz TW, et al. Molecular mechanism of 7TM receptor activation--a global toggle switch model. *Annu Rev Pharmacol Toxicol*. 46(2006):481. [PubMed: 16402913]
26. Pardo L, et al. The role of internal water molecules in the structure and function of the rhodopsin family of G protein-coupled receptors. *Chembiochem*. 2007; 8(1):19. [PubMed: 17173267]
27. Vogel R, et al. Functional role of the "ionic lock"--an interhelical hydrogen-bond network in family A heptahelical receptors. *J Mol Biol*. 2008; 380(4):648. [PubMed: 18554610]
28. Fritze O, et al. Role of the conserved NPxxY(x)5,6F motif in the rhodopsin ground state and during activation. *Proc Natl Acad Sci U S A*. 2003; 100(5):2290. [PubMed: 12601165]
29. Tate CG, Schertler GF. Engineering G protein-coupled receptors to facilitate their structure determination. *Curr Opin Struct Biol*. 2009; 19(4):386. [PubMed: 19682887]
30. Reeves PJ, Kim JM, Khorana HG. Structure and function in rhodopsin: a tetracycline-inducible system in stable mammalian cell lines for high-level expression of opsin mutants. *Proc Natl Acad Sci U S A*. 2002; 99(21):13413. [PubMed: 12370422]
31. Reeves PJ, Callewaert N, Contreras R, Khorana HG. Structure and function in rhodopsin: high-level expression of rhodopsin with restricted and homogeneous N-glycosylation by a tetracycline-inducible N-acetylglucosaminyltransferase I-negative HEK293S stable mammalian cell line. *Proc Natl Acad Sci U S A*. 2002; 99(21):13419. [PubMed: 12370423]
32. Kabsch W. Automatic processing of rotation diffraction data from crystals of initially unknown symmetry and cell constants. *J. Appl. Cryst*. 1993; 26:795.
33. The CCP4 suite: programs for protein crystallography. *Acta Crystallogr D Biol Crystallogr*. 1994; 50(Pt 5):760. [PubMed: 15299374]
34. Emsley P, Cowtan K. Coot: model-building tools for molecular graphics. *Acta Crystallogr D Biol Crystallogr*. 2004; 60(Pt 12 Pt 1):2126. [PubMed: 15572765]
35. Adams PD, et al. PHENIX: building new software for automated crystallographic structure determination. *Acta Crystallogr D Biol Crystallogr*. 2002; 58(Pt 11):1948. [PubMed: 12393927]
36. Alexandrov AI, et al. Microscale fluorescent thermal stability assay for membrane proteins. *Structure*. 2008; 16(3):351. [PubMed: 18334210]
37. McCoy AJ, Grosse-Kunstleve RW, Storoni LC, Read RJ. Likelihood-enhanced fast translation functions. *Acta Crystallogr D Biol Crystallogr*. 2005; 61(Pt 4):458. [PubMed: 15805601]
38. Schuttelkopf AW, van Aalten DM. PRODRG: a tool for high-throughput crystallography of protein-ligand complexes. *Acta Crystallogr D Biol Crystallogr*. 2004; 60(Pt 8):1355. [PubMed: 15272157]
39. Kleywegt GJ. Crystallographic refinement of ligand complexes. *Acta Crystallogr D Biol Crystallogr*. 2007; 63(Pt 1):94. [PubMed: 17164531]

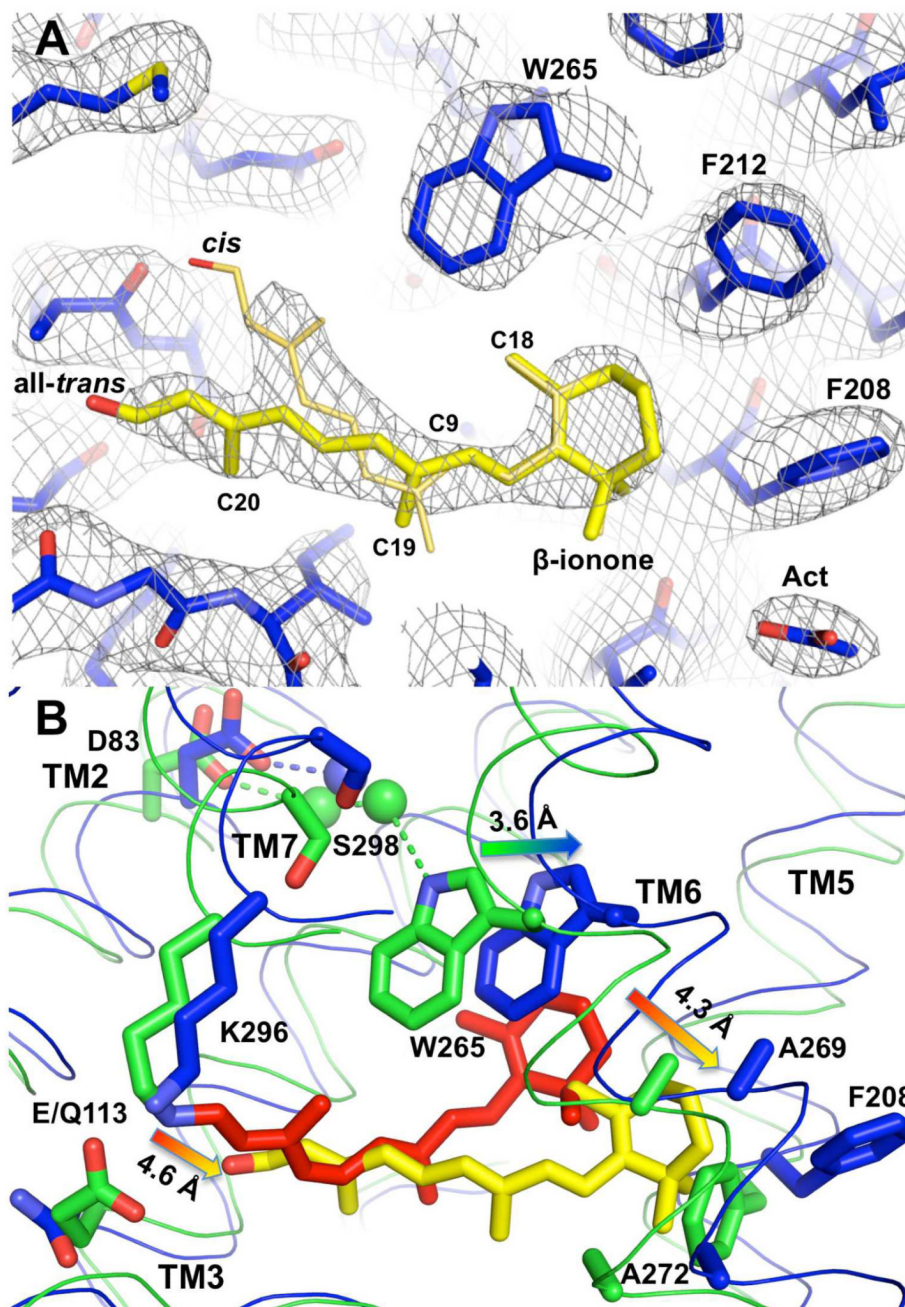


Figure 1. Conformational changes in the retinal binding pocket

A: $2F_o - F_c$ map (contoured at 1.5 sigma) of the retinal-binding pocket. The retinal β -ionone ring is well resolved while density of the polyene chain broadens towards the end facing K296^{7,43}. Occupancy refinements indicated a mixture of 60% all-*trans*-retinal and 40% of isomers rotated around single bonds or double bonds after position C9. An acetate molecule is packed between F208^{5,43} and F276^{6,59} and blocks a potential retinal entry/exit channel².

B: Superposition of E113Q/GaCT (blue, 2 \times 72) with ground state rhodopsin (green, 1GZM)⁷. Compared to the β -ionone ring of 11-*cis*-retinal (red) in ground state rhodopsin, the β -ionone ring of all-*trans*-retinal (yellow) in the active E113Q/GaCT structure is shifted

4.3 Å towards the cleft between TM5 and TM6, where it makes contact with both helices. Simultaneously W265^{6.48} of the CWxP motif is released from its locked position in the ground state, which disrupts a water-mediated interaction to S298^{7.45} and breaks the restraining TM6-TM7 link²⁶. The salt bridge between E113^{3.28} as counterion to the protonated Schiff base and K296^{7.43} is broken in the E113Q/GαCT structure removing a link known to restrain TM3 and TM7 in the inactive, ground-state conformation⁶. By alteration of these three key interactions retinal can induce the rotation of TM6 that opens the G protein-binding site and simultaneously can facilitate a reorganization of hydrogen-bonding networks in the NPxxY and E(D)RY at the cytoplasmic end of TM3 and TM7.

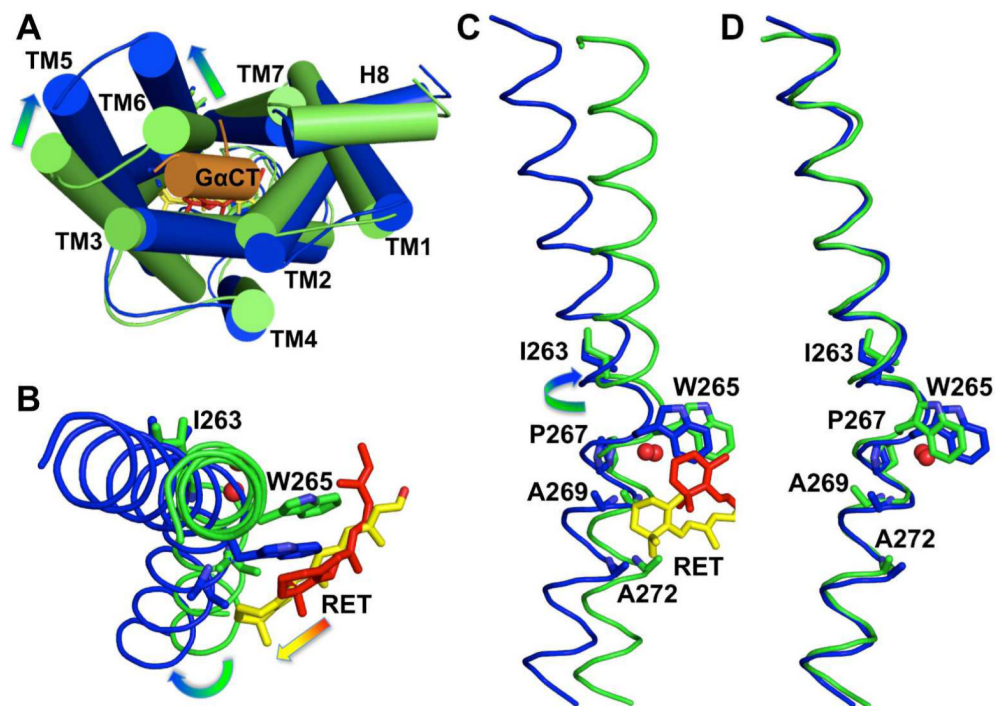


Figure 2. Rearrangement of the heptahelix bundle and rotation of TM6

A: Superposition of C α traces of ground state rhodopsin (green) and E113Q (blue) with bound G protein peptide (orange), as seen from the cytoplasmic side. The main rearrangements of the seven transmembrane helices (cylinders) that open the G protein-binding site are indicated as arrows. The loop regions have been smoothed for clarity. **B, C:** Cytoplasmic and membrane side views of TM6 (C α traces in ribbon representation) from ground state rhodopsin and the E113Q/G α CT structure illustrates how 11-*cis* (red) to all-*trans* (yellow) isomerisation of retinal can release W265^{6,48} from its locked position in the ground state and insert the β -ionone ring between F208^{5,43}/F212^{5,47} in H5 and A269^{6,52}/A272^{6,55} in H6. This leads to a rotation of TM6 that is amplified towards its cytoplasmic end by the characteristic bend of the helix introduced by P267^{6,50} and water⁷. **D:** Superposition of TM6 alone shows that the shape of the helix is preserved during the rearrangements.

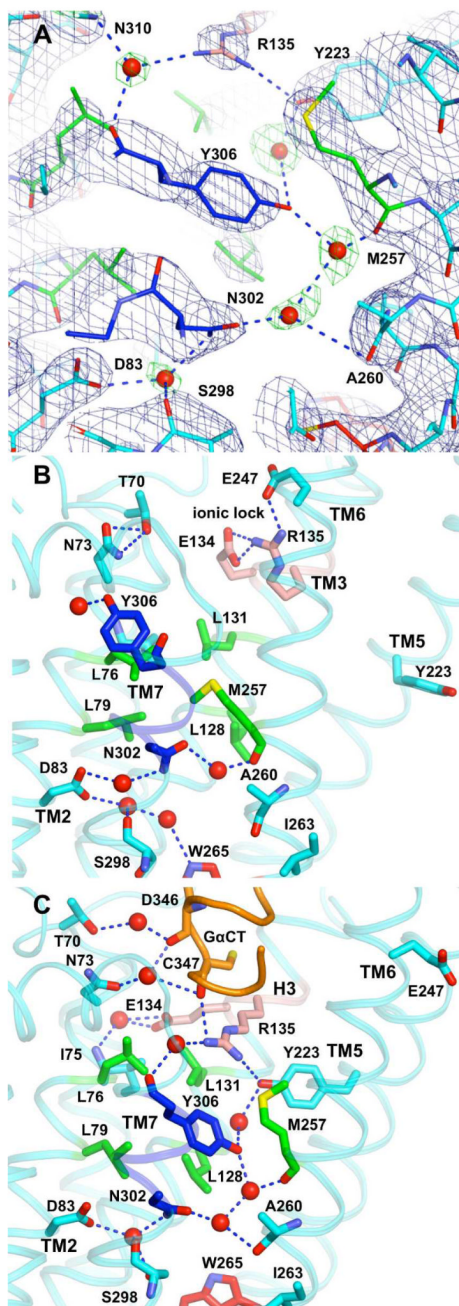


Figure 3. Rearrangement of water mediated hydrogen-bonding networks

A: The E113Q structure reveals potential water mediated hydrogen-bonding networks that connect the retinal-binding region with the GaCT binding site. Strong electron density (Blue mesh represents 2Fo-Fc map contoured at 2.0 sigma. Green mesh shows the Fo-Fc map contoured at 3.0 sigma) difference peaks are observed when waters are omitted during simulated annealing refinement, demonstrating a high degree of local order. **B:** In ground-state rhodopsin, the hydrogen-bonding network connects W265^{6,48} in the retinal-binding pocket with N302^{7,49} of the NPxxY motif (blue) and the carboxyl of M257^{6,40}, via the conserved residues S298^{7,45} and D83^{2,50}. M257^{6,40} is part of a region called the hydrophobic barrier (green) that separates the ionic lock interaction between the E134^{3,49}/

R135^{3.50} pair in the E(D)RY motif (salmon) of TM3 and E247^{6.30} in TM6. **C:** In the active E113Q/GαCT structure, TM6 is rotated including W265^{6.48}, which breaks the water-mediated link to S298^{7.45} in TM7. The TM1-TM2-TM7 network between N55^{1.50}, D83^{2.50} and S298^{7.45} is reorganized but maintains and stabilizes a similar distortion of TM7 induced by P303^{7.50} of the NPxxY motif (blue)²⁶. The hydrophobic barrier that separates the E(D)RY motif (salmon) in TM3 from the membrane core is opened. Y306^{7.53} of the NPxxY motif (blue) in TM7 and Y223^{5.58} in TM5 rearrange to fill the resulting gap and extend the hydrogen-bonded network towards R135^{3.50} of the E(D)RY motif (salmon). R135^{3.50} is released from its ground state bent interaction with E134^{3.49}, which opens the ionic lock and facilitates the outward movement of TM6 that allows binding of the GαCT peptide (orange ribbon). In the indicated location the water cluster can bridge the retinal-binding core with the cytoplasmic side of the receptor and is directly mediating interactions to the G protein peptide.

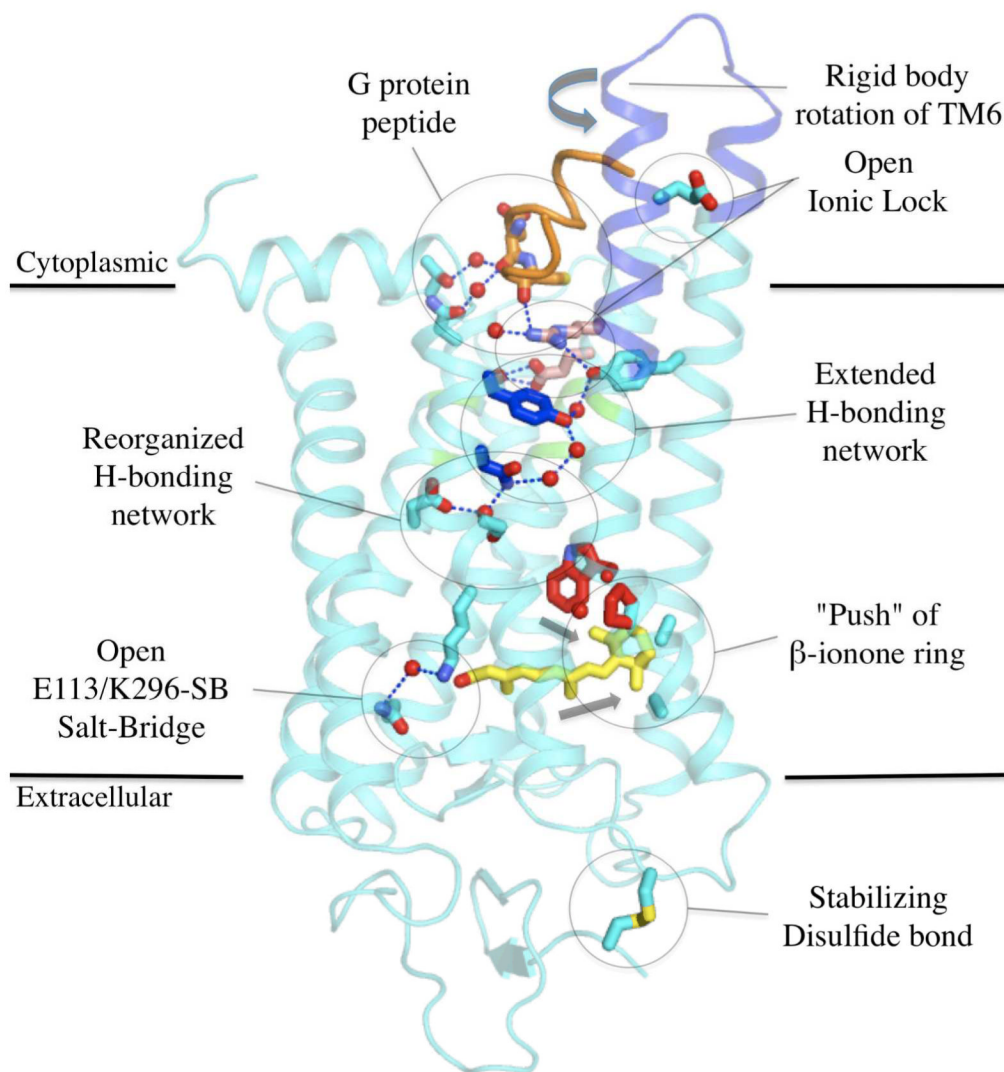


Figure 4. Activation of rhodopsin by the agonist all-*trans*-retinal

The protein backbone of E113Q/G α CT is shown in cyan with predominant conformational changes in TM5 and TM6 (RMSD of C α atoms with respect to 1GZM > 3.5Å) in blue. The key regions involved in rhodopsin activation and discussed in the text are highlighted. The side-chains of the CWxP motif close to the retinal-binding site are coloured red. Side-chains of the NPxxY motif are coloured, blue and extend the hydrogen-bonding network through the green hydrophobic barrier. Side-chains of the E(D)RY motif, as part of the ionic lock and the G protein-binding site are coloured salmon. The G α CT peptide is shown as an orange ribbon. The engineered disulfide bond in the extracellular domain is well isolated from the structural motifs involved in rhodopsin activation, an explanation for its neutral stabilizing characteristics¹⁵.